Letter

Evaluation of multiloop multiscale Feynman integrals for precision physics

Ievgen Dubovyk,[1] Ayres Freitas,[2] Janusz Gluza,[1] Krzysztof Grzanka,[1] Martijn Hidding,[3] and Johann Usovitsch[4]
[1]*Institute of Physics, University of Silesia, Katowice, Poland*
[2]*Pittsburgh Particle physics, Astrophysics and Cosmology Center (PITT PACC), Department of Physics and Astronomy, University of Pittsburgh, Pittsburgh, Pennsylvania 15260, USA*
[3]*Department of Physics and Astronomy, Uppsala University, SE-75120 Uppsala, Sweden*
[4]*Theoretical Physics Department, CERN, 1211 Geneva, Switzerland*

(Received 23 December 2021; accepted 10 October 2022; published 26 December 2022)

Modern particle physics is increasingly becoming a precision science that relies on advanced theoretical predictions for the analysis and interpretation of experimental results. The planned physics program at the LHC and future colliders will require three-loop electroweak and mixed electroweak-QCD corrections to single-particle production and decay processes and two-loop electroweak corrections to pair-production processes. This article presents a new seminumerical approach to multiloop multiscale Feynman integrals calculations which will be able to fill the gap between rigid experimental demands and theory. The approach is based on differential equations with boundary terms specified at Euclidean kinematic points. These Euclidean boundary terms can be computed numerically with high accuracy using sector decomposition or other numerical methods. They are then mapped to the physical kinematic configuration by repeatedly solving the differential equation system in terms of series solutions. An automatic and general method is proposed for constructing a basis of master integrals such that the differential equations are finite. The approach also provides a prescription for the analytic continuation across physical thresholds. Our implementation is able to deliver 8 or more digits of precision, and has a built-in mechanism for checking the accuracy of the obtained results. Its efficacy is illustrated with state-of-the-art examples for three-loop self-energy and vertex integrals and two-loop box integrals.

DOI: 10.1103/PhysRevD.106.L111301

I. INTRODUCTION

With the discovery of the Higgs boson at the Large Hadron Collider (LHC), all building blocks of the Standard Model (SM) have been experimentally confirmed, with the only exception of the Higgs self-coupling, which still awaits direct measurement. However, the SM does not account for important phenomena such as dark matter and the matter-antimatter asymmetry, so that physics beyond the SM is needed. It is reasonable to expect that this new physics couples to the electroweak and/or Higgs sector of the SM, since there are important model-building constraints for couplings to the strong force [1].

Therefore, possible evidence for such new physics can be explored in precision studies of electroweak and Higgs physics at the high-luminosity run of the LHC (HL-LHC) or one of several proposed future e^+e^- colliders: FCC-ee [2], CEPC [3], ILC [4,5], CLIC [6,7]. Through their high integrated luminosities of several ab^{-1}, these machines will be sensitive to very small deviations between the measured value and the SM expectation for a given observable. Thus they can probe extremely feebly coupled new particles or very large new physics scales of tens of TeV.

The SM predictions for these precision analyses are obtained by computing higher-order quantum corrections. At the HL-LHC, some of the most interesting precision studies are Higgs boson production and lepton pair (Drell-Yan) production. For the former, one of the largest sources of theoretical uncertainty stems from mixed QCD-electroweak corrections [8,9]. While some partial results at this order have been computed [10–14], contributions from electroweak diagrams with internal top quarks, both for 3-loop Higgs production and 2-loop Higgs + jet production, are still needed to complete this missing piece. For Drell-Yan production, 2-loop electroweak corrections for the full process $pp \to \ell^+\ell^-$, not just on the Z-boson resonance, are important since LHC measurements cover a broad range of invariant mass [15,16].

Similarly, electroweak 2-loop corrections for several different pair-production processes will be essential for the physics goals of future e^+e^- colliders [17]: $e^+e^- \to W^+W^-$, $e^+e^- \to ZH$, and $e^+e^- \to f\bar{f}$. Measurements of these cross

Published by the American Physical Society under the terms of the Creative Commons Attribution 4.0 International license. Further distribution of this work must maintain attribution to the author(s) and the published article's title, journal citation, and DOI. Funded by SCOAP³.

sections will allow us to determine the W-boson mass with high precision, constrain anomalous couplings between gauge bosons and/or the Higgs boson, and probe heavy neutral vector bosons (Z' bosons). Currently, some results for mixed QCD-electroweak 2-loop corrections are available [18–21], but so far no complete electroweak 2-loop calculation for any pair-production process has been carried out. Even higher-order corrections will be needed for studies of Z-boson production and decay at these future e^+e^- colliders, as well as the indirect prediction of the W-boson mass from the Fermi constant. To match the expected experimental precision, 3-loop and partial 4-loop self-energy and vertex corrections will be required [17,22], which is one order of perturbation theory beyond the current state of the art [23].

It should be emphasized that these are loop corrections in the full SM, involving many massive particles inside the loops. The currently most advanced techniques for analytically computing such multiloop Feynman integrals first reduce them to a small set of master integrals, which then are solved by constructing suitable differential equations (DEs); see Ref. [24] for a recent review. Both of these steps require integration-by-parts (IBP) equation systems [25,26] that become computationally difficult for multiloop integrals with many masses. Instead, one must resort to numerical integration techniques.

The recent calculation of full 2-loop corrections to Z-boson production and decay [23,27,28] made use of numerical evaluations based on sector decomposition (SD) [29–33] and Mellin-Barnes (MB) representations [27,34–38]. However, these methods require large amounts of computing resources and do not always converge to the required level of accuracy, so that a straightforward extension to more loops and/or legs is not possible. Based on previous experience [28], we expect up to 5 digits precision loss due to numerical cancellations between individual loop integrals, so that at least 8 digits of precision are required in many cases for practical applications.

This article introduces an efficient but still very general approach that can be applied to many challenging 2- and 3-loop problems with multiple mass and momentum scales [39]. The key elements are a system of DEs, with boundary terms evaluated at one or more Euclidean (spacelike) kinematic points (which can be reliably determined to high precision with numerical methods). The DEs are then solved, using series expansions, to obtain the final result at the physical Minkowski (timelike) kinematic point. This approach, which is already fully automated in its main parts, will be described in more detail in the next section. In Sec. III we will apply this technique to examples of SM self-energy and vertex Feynman integrals that occur in three-loop Z-decay corrections. The chosen examples are very difficult to evaluate with other analytical or numerical methods. A summary and outlook are given in the final section. Additional examples and implementation details can be found in the Supplemental Material [40].

II. DESCRIPTION OF THE METHOD

Solving Feynman integrals from DEs is an approach initiated in the last decade of the last century [41–44]. Many families of Feynman integrals admit a choice of master integrals for which the system of DEs has a particularly simple "canonical" form [45], which in many cases can be straightforwardly solved in terms of multiple polylogarithms.

More generally, not all Feynman integrals are of polylogarithmic type, and it can become increasingly difficult to find a closed set of analytic functions in terms of which the DEs can be solved. In such cases, one interesting approach, which allows to tackle a wider class of problems, evaluates a set of master integrals by numerically solving a DE system, either in terms of kinematic parameters [46–48] or in terms of an auxiliary mass flow variable [49–51]. In this work, we use the approach of iterated series expansions [52,53], and extend it to make it fully automated. For this purpose, we use the program `DiffExp` [54], which needs as an input a basis of master integrals resulting in a finite system of differential equations. While in several cases a basis was found where the strategy works [55–59], in the present work we construct such a basis in an automatic way. The implementation details of this strategy are presented in the Supplemental Material [40]. When crossing a physical threshold with `DiffExp`, we have to be consistent with the Feynman $i\delta$ prescription. In practice, we consider all unitarity cuts across a diagram topology [60], and for each cut we obtain a linear polynomial of the form $s - M^2$, where s is the square of the momentum flowing across the cut, and M^2 is the square of the sum of the masses of the cut propagators. Each polynomial is assigned a $+i\delta$ prescription and given to `DiffExp`, which allows for the automated crossing of the unitarity cut. We do not search for anomalous thresholds [61,62], which cannot be found by unitarity cuts. This was sufficient for our applications as we did not observe such thresholds during the transport from the Euclidean to the physical region. In general, `DiffExp` will give an error if a singularity is encountered for which a delta prescription is not provided. This way, we manage to fully automate the question of crossing thresholds. In previous studies, it was not discussed how to perform the basis choice and threshold crossing in an automated fashion.

Let us give a brief overview of the method. Consider a basis of master integrals (MIs), $\vec{F}(x,\epsilon)$, depending on a single scale x. We work in dimensional regularization, with $D = 4 - 2\epsilon$ space-time dimensions. We may then derive DEs of the form

$$\frac{d}{dx}\vec{F}(x,\epsilon) = \hat{M}(x,\epsilon)\vec{F}(x,\epsilon), \tag{1}$$

where $\hat{M}(x,\epsilon)$ is a block-triangular matrix. Each block is associated with a sector of integrals. If we denote such a sector by $\vec{f}_i(x,\epsilon)$, we can decompose the DEs in the form

$$\frac{d}{dx}\vec{f}_i(x,\epsilon) = M_i(x,\epsilon)\vec{f}_i(x,\epsilon) + B_i(x,\epsilon)\vec{g}_i(x,\epsilon), \tag{2}$$

where $M_i(x,\epsilon)$ denotes the diagonal block of $\hat{M}(x,\epsilon)$ corresponding to the sector i, and $B_i(x,\epsilon)\vec{g}_i(x,\epsilon)$ captures the off-diagonal terms. One can then expand the integrals and matrices in ϵ:

$$\vec{f}_i(x,\epsilon) = \sum_{j=-k}^{\infty} \vec{f}_i^{(j)}(x,\epsilon)\epsilon^j,$$
$$M_i(x,\epsilon) = \sum_{j=0}^{\infty} M_i^{(j)}(x,\epsilon)\epsilon^j, \tag{3}$$

and solve the system order by order in ϵ. For a given basis, the condition that $M_i(x,\epsilon)$ is finite in ϵ is not always manifest. It is not trivial to find such a finite form, but an algorithmic procedure is provided in the Supplemental Material [40]. For further ideas and software to help facilitate the choice of MIs, see Refs. [63–70].

The DEs system in Eq. (2) fixes the master integrals up to some boundary conditions. It turns out that in the case of our automated DEs approach, a convenient choice for the boundary terms are MIs which are finite in the dimensional regulator ϵ. We use the package `Reduze` [71–74] to identify these MIs. They can be evaluated efficiently for Euclidean kinematics using the method of SD, since only a small number of sectors is needed for finite integrals and no contour deformation is required to avoid Minkowskian thresholds. We employ the package `pySecDec` [30,31] for this purpose. The derivation of a DEs system is done with the help of the IBP reduction program `Kira` [75–78]. With the boundary terms fixed numerically and the DEs system derived analytically, we transport the Euclidean point to the Minkowski point with the aid of the method of series expansions of the DEs system [46,52,53,79] as implemented in `DiffExp` [54].

As demonstrated in the Supplemental Material [40], see therein e.g. in Fig. 4, we may choose different Euclidean points to fix the boundary terms numerically. This allows us to obtain a numerical error estimate of our automated method by taking the difference of two generated results for the same final Minkowski point. A more detailed discussion of the error estimate is provided in the Supplemental Material [40].

Typically, the transport from the Euclidean boundary point to the physical Minkowski kinematics requires several steps since the convergence radius of the series expansion at the boundary point is not large enough to reach the target point. The program `DiffExp` automatically determines the convergence radius and the number of required transport steps.

In general, the complexity of the multiloop computation increases with the number of loops and independent scales and the number of MIs involved. In our automated approach, the largest investment of computing resources is required for the IBP reduction with `Kira` and the numerical evaluation of the boundary terms with `pySecDec`. However, the former needs to be done only once for a given Feynman integral family, and the latter only once for a given choice of mass-parameter values. Our strategy for the transport to the Minkowski region with `DiffExp` automatically deals with thresholds, and it is very fast, so that one can easily evaluate results for multiple different kinematic points, as needed e.g. for phase-space integrations. Quantitative information on the run time for our approach is given in the Supplemental Material [40]. There the reader can also find a description for how our method can be extended to problems with multiple timelike momentum scales.

III. RESULTS AND DISCUSSION

To demonstrate the power and broad applicability of our method, in the following and in the Supplemental Material [40], we present examples for 3-loop self-energy and vertex integrals and 2-loop box integrals. As discussed in the Introduction, these are all examples of key theory ingredients for the physics program of future e^+e^- colliders and/or the HL-LHC. The 3-loop integrals are needed for currently unknown third-order corrections to electroweak precision observables connected with Z-boson production and decay, whereas two-loop box integrals are important to improve the precision of several $2 \to 2$ processes, such as W^+W^-, ZH or $f\bar{f}$ production [82].

The technique described in this article allows one to compute the desired integrals to, in principle, arbitrary order in the dimension regularization parameter $\epsilon = (4-D)/2$ with multidigit precision. To achieve a certain order ϵ^k, some boundary terms need to be evaluated to higher orders $k' > k$ in ϵ. The required order k' is determined automatically from the IBP relations. For the examples shown below, some simple boundary-term integrals have to be computed to $\mathcal{O}(\epsilon^7)$, whereas no more than $\mathcal{O}(\epsilon^3)$ is needed for more complicated boundary terms. When evaluating the boundary terms with SD as implemented in `pySecDec`, the computing time grows approximately linear with the order in ϵ.

All of the following numerical examples are based on the input parameters given in the Supplemental Material [40].

A. Example 1

As part of the 3-loop $\mathcal{O}(\alpha^2\alpha_s)$ corrections to electroweak precision observables, one encounters the following scalar nonplanar self-energy integral with eight propagators and

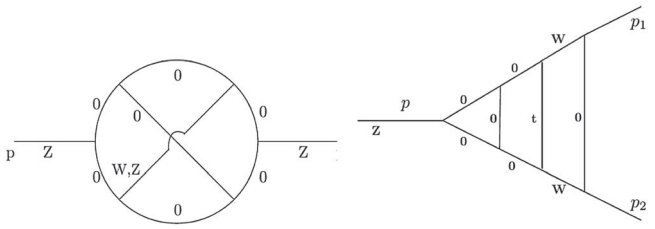

FIG. 1. Three-loop self-energy nonplanar and planar vertex diagrams which correspond to integrals in (4) and (8), respectively. W, Z and t stand for the W boson, Z boson and top quark, respectively.

only one massive W- or Z-boson internal line [85] (see Fig. 1, left):

$$I_{\text{lhNp1}}[D,\{a_i\},p^2,M_a^2] = \int \frac{\mathfrak{D}q_1\mathfrak{D}q_2\mathfrak{D}q_3}{[(q_1-q_2)^2]^{a_1}[q_2^2]^{a_2}} \times \frac{1}{[(q_1-q_3)^2]^{a_3}[(q_2-q_3)^2-M_a^2]^{a_4}[q_3^2]^{a_5}} \times \frac{[q_1^2]^{-a_9}}{[(q_1+p)^2]^{a_6}[(q_1-q_2+p)^2]^{a_7}[(q_3+p)^2]^{a_8}}, \quad (4)$$

where $\mathfrak{D}q_n \equiv \frac{d^D q_n}{i\pi^{D/2}}$ and $a = \text{W, Z}$. This example, for the parameter point $p^2 = M_{\text{Z}}^2$ and $M_a = M_{\text{Z}}$ belongs to a group of integrals which are difficult to evaluate with SD due to threshold effects. Using `pySecDec` with 10^7 integration points we obtain a result with less than two digits precision:

$$I_{\text{lhNp1}}^{\texttt{pySecDec}}[4-2\epsilon,1,1,1,1,1,1,1,1,1,0,M_{\text{Z}}^2,M_{\text{Z}}^2] = 0.460 - 19.164i \pm (0.298 + 0.281i). \quad (5)$$

Increasing the number of integration points does not improve the accuracy substantially. On the other hand, `pySecDec` can deliver accurate results for Euclidean parameter points, $p^2 < 0$, which are used as boundary terms for our automated DEs transport. We thus obtain stable and precise results at the physical point:

$$I_{\text{lhNp1}}[4-2\epsilon,1,1,1,1,1,1,1,1,1,0,M_{\text{Z}}^2,M_{\text{Z}}^2] = -0.000000000 - 19.1262302i + (151.51529 - 150.40641i)\epsilon + \mathcal{O}(\epsilon^2), \quad (6)$$

$$I_{\text{lhNp1}}[4-2\epsilon,1,1,1,1,1,1,1,1,1,0,M_{\text{Z}}^2,M_{\text{W}}^2] = (5.1112260 - 18.5692007i) + (194.660753 - 78.842016i)\epsilon + \mathcal{O}(\epsilon^2). \quad (7)$$

Here and in all the following results, we show all significant digits, i.e. the numerical error only affects digits beyond the ones shown in the equations. The error estimation will be described in more detail in the Supplemental Material [40]. The integral family I_{lhNp1} (4) involves 30 master integrals and is considered simple in the context of our method.

B. Example 2

The next example is a family of 3-loop vertex integrals with one massive top quark and two massive W-boson propagators [see Fig. 1 (right)], defined as

$$I_{\text{vtwPl}}[D,\{a_i\},p^2,M_{\text{W}}^2,m_{\text{t}}^2] = \int \frac{\mathfrak{D}q_1\mathfrak{D}q_2\mathfrak{D}q_3}{[q_3^2-M_{\text{W}}^2]^{a_1}[q_2^2]^{a_2}} \times \frac{1}{[q_1^2]^{a_3}[(q_1-p)^2]^{a_4}[(q_2-p)^2]^{a_5}[(q_3-p)^2-M_{\text{W}}^2]^{a_6}} \times \frac{[(q_1-q_3)^2]^{-a_{10}}[(q_1-p_2)^2]^{-a_{11}}[(q_2-p_2)^2]^{-a_{12}}}{[(q_3-p_1)^2]^{a_7}[(q_2-q_3)^2-m_{\text{t}}^2]^{a_8}[(q_1-q_2)^2]^{a_9}}, \quad (8)$$

where $p = p_1 + p_2$ and $p_1^2 = p_2^2 = 0$. These integrals also appear in so far unknown $\mathcal{O}(\alpha^2\alpha_{\text{s}})$ corrections to Z-pole electroweak precision observables, constituting their most difficult parts.

With `pySecDec` we are unable to obtain a numerical result for the Minkowski point $p^2 = M_{\text{Z}}^2$. The problem already starts with the contour deformation which is necessary for SD with Minkowski kinematics and which fails to complete in a reasonable time. Similar to the SD method, the MB technique fails to deliver high-accuracy results for the considered integrals for $p^2 = M_{\text{Z}}^2$.

Using our automated DEs transport method, the calculation requires the numerical evaluation of 77 master integrals with Euclidean kinematics, $p^2 < 0$, for the boundary terms. For the purpose of the present example, they have been evaluated with `pySecDec` to 10-digit accuracy. After the transport to the physical point $p^2 = M_{\text{Z}}^2$, we get at least 8 significant digits for integrals of the family (8) up to tensor rank-3 (i.e $-3 \le a_{10} + a_{11} + a_{12} \le 0$). We here give numerical result for one rank-3 case:

$$I_{\text{vtwPl}}[1,1,1,1,1,1,1,1,1,-1,-1,-1,M_{\text{Z}}^2,M_{\text{W}}^2,M_{\text{t}}^2] = 0.0833333333/\epsilon^3 + 0.636273147/\epsilon^2 + (0.63462699 + 0.77044487i)/\epsilon + (5.5847828 + 6.1606031i) + \mathcal{O}(\epsilon). \quad (9)$$

Additional examples, a 3-loop self-energy diagram with many massive propagators, and a two-loop box diagram with four scales, are discussed in the Supplemental Material [40].

IV. SUMMARY AND OUTLOOK

In this work, we have proposed an efficient and versatile approach for the evaluation of a wide class of massive multiloop, multiscale Feynman integrals numerically, with typically 8 or more digits precision. It is based on the method of DEs with boundary terms specified for Euclidean kinematics, which are transported to the physical Minkowski kinematics using series solutions of the DEs. The Euclidean boundary-term integrals avoid all threshold singularities and thus can be straightforwardly evaluated numerically. Our implementation combines the public programs `Kira`, `Reduze`, `pySecDec` and `DiffExp` in a way that allows us to automatically construct the required integral families and the transport from the Euclidean boundary point to the physical kinematic point, including the analytical continuation across thresholds.

In principle, the technique can be extended to higher numerical accuracy and to wider classes of integrals with more loops and more external legs. A major bottleneck are the IBP reductions that are needed to construct the DEs system. A significant speed-up of this step is achieved when using numerical values for the relevant mass and kinematic parameters. In addition, the evaluation of the boundary terms for Euclidean kinematics can be time-consuming if a high level of precision is required. Fortunately, there are ongoing improvements to the SD and MB methods; see e.g. Refs. [31,86,87]. In this respect, also new public packages based exclusively on DEs can be directly applied [88,89].

It is worth mentioning that the 3-loop examples presented in this article are very difficult to solve with existing analytical techniques (e.g. using IBP and DEs) and general numerical methods (such as SD or MB methods). The proposed new technique is sufficiently general to provide the foundation for the computation of the required 3-loop corrections needed for electroweak and Higgs precision studies at the HL-LHC and future e^+e^- colliders, which are key elements of the physics program of these machines [9,22]. Other applications include flavor physics at Belle-II and low-energy precision tests of the Standard Model.

ACKNOWLEDGMENTS

This work has been supported in part by the Polish National Science Center (NCN) under Grant No. 2017/25/B/ST2/01987, the Research Excellence Initiative of the University of Silesia in Katowice, the U.S. National Science Foundation under Grants No. PHY-1820760 and No. PHY-2112829. M. H. is supported by the European Research Council under Grant No. ERC-STG-804286 UNISCAMP.

[1] A new physics particle with renormalizable QCD couplings but no weak or Higgs interactions would be stable and thus cosmologically excluded.
[2] A. Abada *et al.*, FCC-ee: The lepton collider: Future circular collider conceptual design report volume 2, Eur. Phys. J. Special Topics **228**, 261 (2019).
[3] J. Guimarães da Costa, Y. Gao, S. Jin, J. Qian, C. Tully, C. Young, L. Wang, M. Ruan, H. Zhu, Q. Ouyang *et al.* (CEPC Study Group), CEPC conceptual design report: Volume 2—physics & detector, arXiv:1811.10545.
[4] H. Baer, T. Barklow, K. Fujii, Y. Gao, A. Hoang, S. Kanemura, J. List, H. E. Logan, A. Nomerotski, M. Perelstein *et al.*, The international linear collider technical design report—volume 2: Physics, arXiv:1306.6352.
[5] P. Bambade *et al.*, The international linear collider: A global project, arXiv:1903.01629.
[6] L. Linssen, A. Miyamoto, M. Stanitzki, and H. Weerts, Physics and detectors at CLIC: CLIC conceptual design report, 2012, 10.5170/CERN-2012-003.
[7] T. Charles *et al.*, The compact linear collider (CLIC)—2018 summary report 2/2018, Report No. CERN-2018-005-M, 2018, 10.23731/CYRM-2018-002.
[8] C. Anastasiou, R. Boughezal, and F. Petriello, Mixed QCD-electroweak corrections to Higgs boson production in gluon fusion, J. High Energy Phys. 04 (2009) 003.
[9] C. Anastasiou, C. Duhr, F. Dulat, E. Furlan, T. Gehrmann, F. Herzog, A. Lazopoulos, and B. Mistlberger, High precision determination of the gluon fusion Higgs boson cross-section at the LHC, J. High Energy Phys. 05 (2016) 058.
[10] M. Bonetti, K. Melnikov, and L. Tancredi, Three-loop mixed QCD-electroweak corrections to Higgs boson gluon fusion, Phys. Rev. D **97**, 034004 (2018).
[11] C. Anastasiou, V. del Duca, E. Furlan, B. Mistlberger, F. Moriello, A. Schweitzer, and C. Specchia, Mixed QCD-electroweak corrections to Higgs production via gluon fusion in the small mass approximation, J. High Energy Phys. 03 (2019) 162.
[12] M. Bonetti, E. Panzer, V. A. Smirnov, and L. Tancredi, Two-loop mixed QCD-EW corrections to $gg \to Hg$, J. High Energy Phys. 11 (2020) 045.
[13] M. Becchetti, R. Bonciani, V. Del Duca, V. Hirschi, F. Moriello, and A. Schweitzer, Next-to-leading order corrections to light-quark mixed QCD-EW contributions to Higgs boson production, Phys. Rev. D **103**, 054037 (2021).
[14] M. Becchetti, F. Moriello, and A. Schweitzer, Two-loop amplitude for mixed QCD-EW corrections to $gg \to Hg$, J. High Energy Phys. 04 (2022) 139.

[15] ATLAS Collaboration, Measurement of the effective leptonic weak mixing angle using electron and muon pairs from Z-boson decay in the ATLAS experiment at $\sqrt{s} = 8$ TeV, ATLAS-CONF-2018-037, 2018, http://cds.cern.ch/record/2630340.

[16] A. M. Sirunyan *et al.*, Measurement of the weak mixing angle using the forward-backward asymmetry of Drell-Yan events in pp collisions at 8 TeV, Eur. Phys. J. C **78**, 701 (2018).

[17] A. Freitas *et al.*, Theoretical uncertainties for electroweak and Higgs-boson precision measurements at FCC-ee, arXiv:1906.05379.

[18] Y. Gong, Z. Li, X. Xu, L. L. Yang, and X. Zhao, Mixed QCD-EW corrections for Higgs boson production at e^+e^- colliders, Phys. Rev. D **95**, 093003 (2017).

[19] Q.-F. Sun, F. Feng, Y. Jia, and W.-L. Sang, Mixed electroweak-QCD corrections to $e + e- \to$ HZ at Higgs factories, Phys. Rev. D **96**, 051301 (2017).

[20] M. Heller, A. von Manteuffel, R. M. Schabinger, and H. Spiesberger, Mixed EW-QCD two-loop amplitudes for $q\bar{q} \to \ell^+\ell^-$ and γ_5 scheme independence of multi-loop corrections, J. High Energy Phys. 05 (2021) 213.

[21] R. Bonciani, L. Buonocore, M. Grazzini, S. Kallweit, N. Rana, F. Tramontano, and A. Vicini, Mixed Strong-Electroweak Corrections to the Drell-Yan Process, Phys. Rev. Lett. **128**, 012002 (2022).

[22] A. Blondel *et al.*, Standard model theory for the FCC-ee Tera-Z stage, Vol. 3/2019 of CERN Yellow Reports: Monographs, CERN, Geneva, Report Nos. CERN-2019-003, BU-HEPP-18-04, CERN-TH-2018-145, IFJ-PAN-IV-2018-09, KW 18-003, MITP/18-052, MPP-2018-143, SI-HEP-2018-21, 2018, 10.23731/CYRM-2019-003.

[23] I. Dubovyk, A. Freitas, J. Gluza, T. Riemann, and J. Usovitsch, Electroweak pseudo-observables and Z-boson form factors at two-loop accuracy, J. High Energy Phys. 08 (2019) 113.

[24] A. V. Kotikov, Differential equations and Feynman integrals, in *Antidifferentiation and the Calculation of Feynman Amplitudes* (Springer, 2021), 10.1007/978-3-030-80219-6_10.

[25] K. Chetyrkin and F. Tkachov, Integration by parts: The algorithm to calculate β functions in 4 loops, Nucl. Phys. **B192**, 159 (1981).

[26] S. Laporta, High precision calculation of multiloop Feynman integrals by difference equations, Int. J. Mod. Phys. A **15**, 5087 (2000).

[27] I. Dubovyk, A. Freitas, J. Gluza, T. Riemann, and J. Usovitsch, The two-loop electroweak bosonic corrections to $\sin^2\theta^{\rm b}_{\rm eff}$, Phys. Lett. B **762**, 184 (2016).

[28] I. Dubovyk, A. Freitas, J. Gluza, T. Riemann, and J. Usovitsch, Complete electroweak two-loop corrections to Z boson production and decay, Phys. Lett. B **783**, 86 (2018).

[29] T. Binoth and G. Heinrich, An automatized algorithm to compute infrared divergent multi-loop integrals, Nucl. Phys. **B585**, 741 (2000).

[30] S. Borowka, G. Heinrich, S. Jahn, S. P. Jones, M. Kerner, J. Schlenk, and T. Zirke, pySecDec: A toolbox for the numerical evaluation of multi-scale integrals, Comput. Phys. Commun. **222**, 313 (2018).

[31] S. Borowka, G. Heinrich, S. Jahn, S. P. Jones, M. Kerner, and J. Schlenk, A GPU compatible quasi-Monte Carlo integrator interfaced to pySecDec, Comput. Phys. Commun. **240**, 120 (2019).

[32] A. V. Smirnov and M. N. Tentyukov, Feynman Integral Evaluation by a Sector decomposiTion Approach (FIESTA), Comput. Phys. Commun. **180**, 735 (2009).

[33] A. V. Smirnov, FIESTA 4: Optimized Feynman integral calculations with GPU support, Comput. Phys. Commun. **204**, 189 (2016).

[34] J. Gluza, K. Kajda, and T. Riemann, AMBRE: A *Mathematica* package for the construction of Mellin-Barnes representations for Feynman integrals, Comput. Phys. Commun. **177**, 879 (2007).

[35] M. Czakon, Automatized analytic continuation of Mellin-Barnes integrals, Comput. Phys. Commun. **175**, 559 (2006).

[36] J. Usovitsch, Numerical evaluation of Mellin-Barnes integrals in Minkowskian regions and their application to two-loop bosonic electroweak contributions to the weak mixing angle of the $Z\bar{b}b$-vertex, Ph.D. thesis, Humboldt-Universität zu Berlin, Inst. Math., 2018.

[37] I. Dubovyk, J. Gluza, T. Riemann, and J. Usovitsch, Numerical integration of massive two-loop Mellin-Barnes integrals in Minkowskian regions, Proc. Sci., LL2016 (**2016**) 034 [arXiv:1607.07538].

[38] J. Usovitsch, I. Dubovyk, and T. Riemann, MBnumerics: Numerical integration of Mellin-Barnes integrals in physical regions, Proc. Sci., LL2018 (**2018**) 046 [arXiv:1810.04580].

[39] In principle, it is also applicable at higher loop orders, but we have not studied any examples beyond three loops.

[40] See Supplemental Material at http://link.aps.org/supplemental/10.1103/PhysRevD.106.L111301 for input parameters, additional examples, e.g. a 2-loop four-scale box diagram, and miscellaneous implementational details and remarks for a more detailed discussion of the method.

[41] A. Kotikov, Differential equations method: New technique for massive Feynman diagrams calculation, Phys. Lett. B **254**, 158 (1991).

[42] A. Kotikov, Differential equations method: The calculation of vertex type Feynman diagrams, Phys. Lett. B **259**, 314 (1991).

[43] A. V. Kotikov, Differential equation method: The calculation of N point Feynman diagrams, Phys. Lett. B **267**, 123 (1991).

[44] E. Remiddi, Differential equations for Feynman graph amplitudes, Nuovo Cimento A **110**, 1435 (1997).

[45] J. M. Henn, Multiloop Integrals in Dimensional Regularization Made Simple, Phys. Rev. Lett. **110**, 251601 (2013).

[46] S. Pozzorini and E. Remiddi, Precise numerical evaluation of the two loop sunrise graph master integrals in the equal mass case, Comput. Phys. Commun. **175**, 381 (2006).

[47] M. K. Mandal and X. Zhao, Evaluating multi-loop Feynman integrals numerically through differential equations, J. High Energy Phys. 03 (2019) 190.

[48] M. L. Czakon and M. Niggetiedt, Exact quark-mass dependence of the Higgs-gluon form factor at three loops in QCD, J. High Energy Phys. 05 (2020) 149.

[49] X. Liu, Y.-Q. Ma, and C.-Y. Wang, A systematic and efficient method to compute multi-loop master integrals, Phys. Lett. B **779**, 353 (2018).

[50] X. Liu and Y.-Q. Ma, Determining arbitrary Feynman integrals by vacuum integrals, Phys. Rev. D **99**, 071501 (2019).
[51] C. Brønnum-Hansen and C.-Y. Wang, Contribution of third generation quarks to two-loop helicity amplitudes for W boson pair production in gluon fusion, J. High Energy Phys. 01 (2021) 170.
[52] F. Moriello, Generalised power series expansions for the elliptic planar families of Higgs + jet production at two loops, J. High Energy Phys. 01 (2020) 150.
[53] R. Bonciani, V. Del Duca, H. Frellesvig, J. M. Henn, M. Hidding, L. Maestri, F. Moriello, G. Salvatori, and V. A. Smirnov, Evaluating a family of two-loop non-planar master integrals for Higgs + jet production with full heavy-quark mass dependence, J. High Energy Phys. 01 (2020) 132.
[54] M. Hidding, DiffExp, a *Mathematica* package for computing Feynman integrals in terms of one-dimensional series expansions, Comput. Phys. Commun. **269**, 108125 (2021).
[55] S. Badger, H. B. Hartanto, J. Kryś, and S. Zoia, Two-loop leading colour helicity amplitudes for $W^{\pm}\gamma + j$ production at the LHC, J. High Energy Phys. 05 (2022) 035.
[56] T. Armadillo, R. Bonciani, S. Devoto, N. Rana, and A. Vicini, Two-loop mixed QCD-EW corrections to neutral current Drell-Yan, J. High Energy Phys. 05 (2022) 072.
[57] D. Chicherin, V. Sotnikov, and S. Zoia, Pentagon functions for one-mass planar scattering amplitudes, J. High Energy Phys. 01 (2022) 096.
[58] S. Badger, H. B. Hartanto, J. Kryś, and S. Zoia, Two-loop leading-colour QCD helicity amplitudes for Higgs boson production in association with a bottom-quark pair at the LHC, J. High Energy Phys. 11 (2021) 012.
[59] S. Abreu, H. Ita, B. Page, and W. Tschernow, Two-loop hexa-box integrals for non-planar five-point one-mass processes, J. High Energy Phys. 03 (2022) 182.
[60] R. E. Cutkosky, Singularities and discontinuities of Feynman amplitudes, J. Math. Phys. (N.Y.) **1**, 429 (1960).
[61] L. D. Landau, On analytic properties of vertex parts in quantum field theory, Nucl. Phys. **13**, 181 (1959).
[62] N. Nakanishi, Ordinary and anomalous thresholds in perturbation theory, Prog. Theor. Phys. **22**, 128 (1959).
[63] M. Prausa, epsilon: A tool to find a canonical basis of master integrals, Comput. Phys. Commun. **219**, 361 (2017).
[64] O. Gituliar and V. Magerya, Fuchsia: A tool for reducing differential equations for Feynman master integrals to epsilon form, Comput. Phys. Commun. **219**, 329 (2017).
[65] A. von Manteuffel and L. Tancredi, A non-planar two-loop three-point function beyond multiple polylogarithms, J. High Energy Phys. 06 (2017) 127.
[66] L. Adams, E. Chaubey, and S. Weinzierl, Simplifying Differential Equations for Multiscale Feynman Integrals beyond Multiple Polylogarithms, Phys. Rev. Lett. **118**, 141602 (2017).
[67] J. Henn, B. Mistlberger, V. A. Smirnov, and P. Wasser, Constructing d-log integrands and computing master integrals for three-loop four-particle scattering, J. High Energy Phys. 04 (2020) 167.
[68] C. Dlapa, J. Henn, and K. Yan, Deriving canonical differential equations for Feynman integrals from a single uniform weight integral, J. High Energy Phys. 05 (2020) 025.
[69] J. Usovitsch, Factorization of denominators in integration-by-parts reductions, arXiv:2002.08173.
[70] A. V. Smirnov and V. A. Smirnov, How to choose master integrals, Nucl. Phys. **B960**, 115213 (2020).
[71] E. Panzer, Feynman integrals and hyperlogarithms, Ph.D. thesis, Humboldt University, 2015, https://edoc.hu-berlin.de/handle/18452/17809.
[72] A. von Manteuffel, E. Panzer, and R. M. Schabinger, A quasi-finite basis for multi-loop feynman integrals, J. High Energy Phys. 02 (2015) 120.
[73] A. von Manteuffel, E. Panzer, and R. M. Schabinger, Computation of form factors in massless QCD with finite master integrals, Phys. Rev. D **93**, 125014 (2016).
[74] A. von Manteuffel and C. Studerus, Reduze 2—Distributed Feynman integral reduction, arXiv:1201.4330.
[75] P. Maierhöfer, J. Usovitsch, and P. Uwer, Kira—a Feynman integral reduction program, Comput. Phys. Commun. **230**, 99 (2018).
[76] J. Klappert, F. Lange, P. Maierhöfer, and J. Usovitsch, Integral reduction with Kira 2.0 and finite field methods, Comput. Phys. Commun. **266**, 108024 (2021).
[77] J. Klappert and F. Lange, Reconstructing rational functions with FireFly, Comput. Phys. Commun. **247**, 106951 (2020).
[78] J. Klappert, S. Y. Klein, and F. Lange, Interpolation of dense and sparse rational functions and other improvements in FireFly, Comput. Phys. Commun. **264**, 107968 (2021).
[79] See also Ref. [80,81] for a similar approach for single-scale problems.
[80] R. N. Lee, A. V. Smirnov, and V. A. Smirnov, Evaluating 'elliptic' master integrals at special kinematic values: Using differential equations and their solutions via expansions near singular points, J. High Energy Phys. 07 (2018) 102.
[81] M. Fael, F. Lange, K. Schönwald, and M. Steinhauser, A semi-analytic method to compute Feynman integrals applied to four-loop corrections to the $\overline{\text{MS}}$-pole quark mass relation, J. High Energy Phys. 09 (2021) 152.
[82] See Refs. [83,84] for recent independent efforts on electroweak two-loop box integrals.
[83] Q. Song and A. Freitas, On the evaluation of two-loop electroweak box diagrams for $e^+e^- \to HZ$ production, J. High Energy Phys. 04 (2021) 179.
[84] X. Liu and Y.-Q. Ma, Multiloop corrections for collider processes using auxiliary mass flow, Phys. Rev. D **105**, L051503 (2022).
[85] In this and the following examples, the large number of massless propagators occurs because all SM fermions except the top quark are taken to be massless.
[86] M. Borinsky, Tropical Monte Carlo quadrature for Feynman integrals, arXiv:2008.12310.
[87] B. Ananthanarayan, S. Banik, S. Friot, and S. Ghosh, Multiple Series Representations of N-fold Mellin-Barnes Integrals, Phys. Rev. Lett. **127**, 151601 (2021).
[88] X. Liu and Y.-Q. Ma, AMFlow: A *Mathematica* package for Feynman integrals computation via Auxiliary Mass Flow, arXiv:2201.11669.
[89] T. Armadillo, R. Bonciani, S. Devoto, N. Rana, and A. Vicini, Evaluation of Feynman integrals with arbitrary complex masses via series expansions, Comput. Phys. Commun. **282**, 108545 (2023).